J. Pestic. Sci. **49**(2), 114–121 (2024)
DOI: 10.1584/jpestics.D23-062

JOURNAL OF PESTICIDE SCIENCE

Brief Report

Selective detection of paraquat by a cucurbit[7]uril-based fluorescent probe

Pei-Hui Shan,[1] Ding-Wu Pan,[1] Chun-Rong Li,[2,*] Tie-Hong Meng,[2] Carl Redshaw,[3,*] Zhu Tao[1] and Xin Xiao[1,*]

[1] *Key Laboratory of Macrocyclic and Supramolecular Chemistry of Guizhou Province, Guizhou University, Guiyang 550025, China*
[2] *Public Course Teaching Department, Qiannan Medical College for Nationalities, Duyun, 558000, China*
[3] *Chemistry, School of Natural Sciences, University of Hull, Hull HU6 7RX, U.K.*

(Received November 14, 2023; Accepted January 21, 2024)

Supplementary material

A simple fluorescent "on-off" system that can be utilized for the selective identification and determination of paraquat (PQ) is presented herein. ^{1}H NMR spectroscopic data indicated that in aqueous solution the alkaloid palmatine can be partially encapsulated within the cucurbit[7]uril (Q[7]) cavity, whereby a stable 1 : 1 host–guest inclusion complex is formed. Other characterization techniques including mass spectrometry, UV-Vis and fluorescence spectroscopy also provided further evidence, and the host-guest inclusion complex was found to exhibit reasonable fluorescence intensity. It is noteworthy that the addition of PQ resulted in quenching the fluorescence of the host-guest inclusion complex, whereas the presence of 12 other pesticides did not significantly affect the fluorescence intensity. Given the linear relationship between the intensity of the fluorescence and the PQ concentration, the PQ concentration in aqueous solution was easily detected. Thus, a new method for identifying and determining the fluorescence quenching of PQ has been developed in this work.

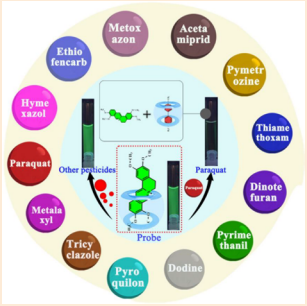

Keywords: cucurbit[*n*]urils, supramolecular assembly, selective recognition, fluorescent probe, host–guest chemistry.

Introduction

Quality of life and the health of the planet are major issues in the modern era. The use of chemicals is ubiquitous in modern day life, and the increasing reliance on pesticides in today's agriculture poses a real threat to both the environment and to food safety.[1)] Given such issues, the detection of these highly toxic compounds is crucial for human health. One toxic agrochemical worthy of attention is paraquat, 1,1-dimethyl-4,4-bipyridyl dichloride (PQ), which sees widespread use given its high herbicidal efficacy and useful weed control properties.[2)] Unfortunately, PQ possesses very high solubility in water, and this means that residual paraquat, particularly after overuse, can readily enter the environment and impact on fish and other organisms. It can also affect human health *via* drinking water and can lead to food contamination. Indeed, the extremely toxic nature of PQ means that it is potentially lethal to both animals and humans.[3)] What makes matters worse, is that there is no effective antidote for PQ, which consequently may result in a high mortality rate. A number of paraquat-targeting sensors have appeared in the literature in recent years, with the sensing devices varying from molecular organics to nanomaterials.[4–10)] However, these methods typically require sophisticated instrumentation, long response times, cumbersome sample preparations, or skilled data analysts, all of which severely limits their application in field testing.

Cucurbit[*n*]urils (*n*=5–8, 10, 13–15) are herein abbreviated as Q[*n*]s and consist of *n* glycoluril units linked by 2*n* methylene bridges and possess hydrophobic cavities and polar carbonyl oxygens at the portal (Fig. 1).[11–16)] In previous studies, it has been shown that cucurbiturils are capable of binding to a range of guests in aqueous solution, including organic molecules, metal

* To whom correspondence should be addressed.
E-mail: lichunrong68@163.com, C.Redshaw@hull.ac.uk, gyhxxiaoxin@163.com
Published online March 23, 2024

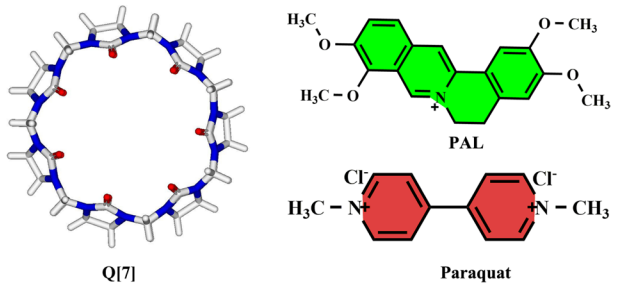

Fig. 1. The molecular structures of Q[7], PAL and the pesticide paraquat (PQ).

ions, amino acids, peptides as well as some pesticides.[17–29] The isoquinoline alkaloid palmatine hydrochloride (PAL) due to its structural peculiarities does not exhibit intrinsic fluorescence in aqueous environments. By contrast, following the interaction of PAL with Q[7], the resulting host–guest complex emits a moderately intense fluorescence.[30,31] With this in mind, we note the widespread use of fluorescence sensing for the detection of various substances, where the attraction is the simplicity, operability, and sensitivity of the method.[32–44] Examples include Li *et al.*, who have utilized a fluorescent probe constructed using Q[7] and PAL in order to detect ethambutol.[45] Also, Yang *et al.* reported a fluorescent probe constructed using Q[7] and PAL for the detection of *L*-cystine.[46] In the field of cucurbit[*n*]urils, many fluorescent probes have appeared in the literature constructed from PAL/Q[*n*] for the detection of a variety of small molecules,[47–51] however few seem to be available for the detection of pesticides. Based on this, we decided to explore if the PAL probe could be encapsulated within the cavity of Q[7] and thereby form an inclusion complex and also if Q[7]-PAL can subsequently be employed for pesticide detection.

In this study, the binding ability of Q[7] to PAL was investigated by employing a variety of techniques, including ^{1}H NMR, UV-vis and fluorescence spectroscopies, and isothermal titration calorimetry (ITC). These studies revealed the formation of a 1:1 host–guest inclusion complex that exhibited moderate fluorescence. Importantly, there was significant quenching of the fluorescence intensity of the inclusion complex on addition of paraquat (PQ) (Fig. 1) to the host-guest (1:1) inclusion complex Q[7]@PAL. By contrast, on addition of 12 other pesticides (Fig. S1) namely Metalaxyl, Tricyclazole, Pyroquilon, Dodine, Pyrimethanil, Dinotefuran, Thiamethoxam, Pymetrozine, Acetamiprid, Metoxazon, Ethiofencarb, Hymexazol to the same inclusion complex, there were no significant changes in the fluorescence. These results suggested that this system can be utilized for the selective detection and determination of PQ in an aqueous environment. Moreover, the method is characterized by a fast response, high sensitivity and a readable signal output. We note that the inclusion of PQ (and Diquat) with both Q[7] and Q[8] has previously been investigated. Results revealed a good complementarity between Q[7] and PQ which afforded higher stability.[52]

Materials and methods

1. *Instruments*

The absorption spectra of the host-guest complexes were recorded on an Aglient 8453 spectrophotometer at room temperature. The fluorescence spectra were obtained using a Varian RF-540 fluorescence spectrophotometer. The excitation and emission slit width was 5 nm, the voltage was 600 V and the excitation wavelength was 343 nm. All NMR spectroscopic data were recorded on a Bruker DPX 400 spectrometer in D_2O (pD=2) at 293.15 K. ITC was performed in aqueous solutions at atmospheric pressure and 298.15 K by using a Nano ITC (TA, USA). Each solution was degassed and thermostated by a ThermoVac accessory prior to the titration experiment. A constant volume of Q[7] solution in a 0.250 mL syringe was injected into a reaction cell (1.4227 mL) containing a solution of PAL in the same aqueous solution. Computer simulations were performed using Nano ITC analyze software.

2. *Reagents and chemicals*

The Q[7] used in the experiments was prepared according to the literature method.[53] PAL and the pesticides used were obtained commercially and were used without further purification. Working standard solutions were generated by diluting stock standard solutions with double-distilled water prior to use. All other chemicals used were of analytical reagent grade. Double distilled water was used throughout.

Results

1. *Formation of 1:1 inclusion complexes in aqueous solution*

To shed some light on the binding characteristics associated with the interaction between Q[7] and PAL in aqueous solution, ^{1}H NMR spectroscopic titration experiments were employed. The ^{1}H NMR spectra of PAL in neutral D_2O solutions, both with

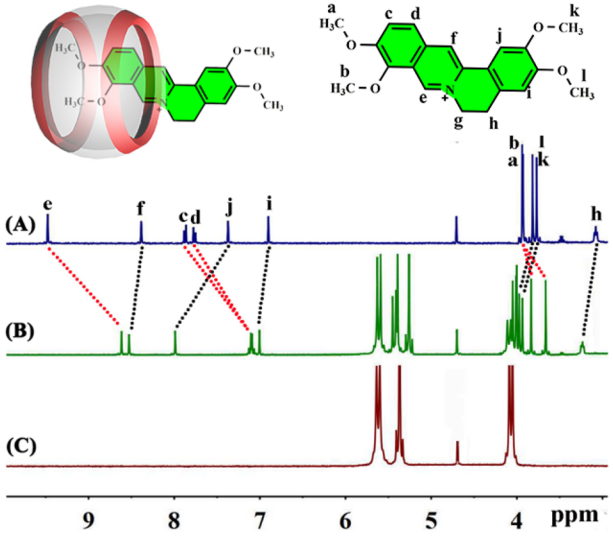

Fig. 2. ^{1}H NMR spectra of PAL (2.0 mmol/L) in the absence (A) and presence of 1.02 eq of Q[7] (B) and neat Q[7] (C) in D_2O at 20°C.

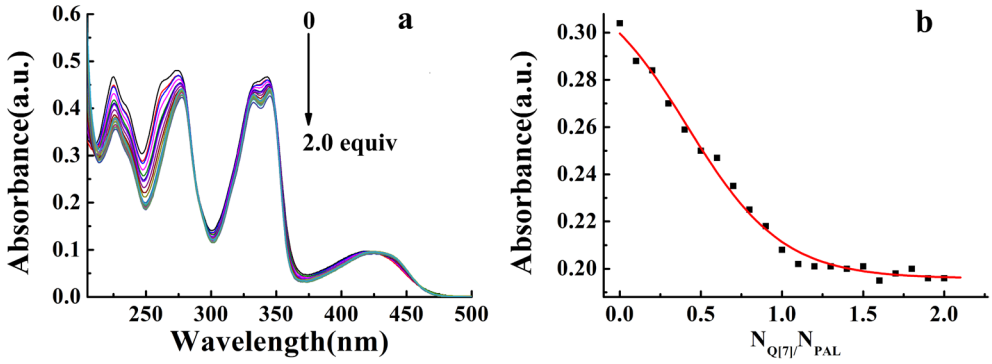

Fig. 3. (a) UV-vis titration of PAL (2×10^{-5} mol·L^{-1}) with increasing concentrations of Q[7]; (b) absorbance (A) *vs.* ratio of number of mol of host and guest $N_{Q[7]}/N_{PAL}$.

and without different equivalents of Q[7] present, are depicted in Fig. 2. Significant shifts were evident for the PAL protons Ha, Hb Hc, Hd and He as Q[7] was added, whilst significant downfield shifts were observed for the protons PAL Hf, Hi and Hj. These spectroscopic observations can be rationalized in terms of encapsulation of the methoxyisoquinoline motif, with the functionalized benzene ring remaining in an external position.

2. UV-vis and fluorescence spectroscopy

The binding ability of Q[7] with PAL was next investigated by the use of both UV-vis (Fig. 3) and fluorescence (Fig. 4) spectroscopic titration experiments in aqueous solution. It is evident from Fig. 3a that the characteristic absorption peaks (225, 274 and 343 nm) of PAL are present. The guest absorption peak exhibited a red-shift to 279 nm as Q[7] was added. Concomitantly, a pronounced decrease in the PAL absorbance was observed, suggestive of high binding affinity between Q[7] and PAL. By using the molar ratio method (Fig. 3b), a 1:1 binding model produced a good fit, and this 1:1 stoichiometry was further confirmed by a continuous variation Job's plot (Fig. S2).

Moreover, as Q[7] is added, the PAL fluorescence spectrum also exhibits significant changes. It is known that in aqueous solution the guest is not itself fluorescent, however on slow addition of Q[7], the fluorescence emission of PAL was significantly enhanced at λ_{em}=491 nm as shown in Fig. 4a. At the same time, with the continuous addition of Q[7], when the stoichiometric ratio of Q[7]:PAL was 1:1, the change in the fluorescence intensity of the system tended to be weaker, and the whole system reached equilibrium (Fig. 4b), which is associated with the formation of the 1:1 host–guest inclusion complex. In this system, the guest is provided with a micro hydrophobic environment by the Q[7] host.[54,55]

3. ITC

To glean more information about the Q[7]/PAL interaction, ambient temperature ITC experiments (Fig. S3) were conducted in a neutral aqueous solution. It is clear also from Fig. S3, where ΔH = −29.14 kJ·mol^{-1}, $T\Delta S$=5.40 kJ·mol^{-1}, ΔG = −34.54 kJ·mol^{-1}, that enthalpy and entropy each contribute to host–guest complex formation. This is thought to result partly from an ionic dipole interaction involving the PAL positively charged nitrogen centres and portal oxygens of the host, with a favourable enthalpy resulting from van der Waals interactions of the PAL surface and the Q[7] inner wall. It is also likely that the removal of cavity and portal water molecules together with those associated with the dissolved PAL shell will contribute to the increased entropy. By using the enthalpy and entropy values and the van't Hoff equation ($\ln K = -\Delta H/RT + \Delta S/R$), the binding constant for the Q[7]/PAL system was calculated at $(1.12\pm0.2)\times10^5$ M^{-1}.

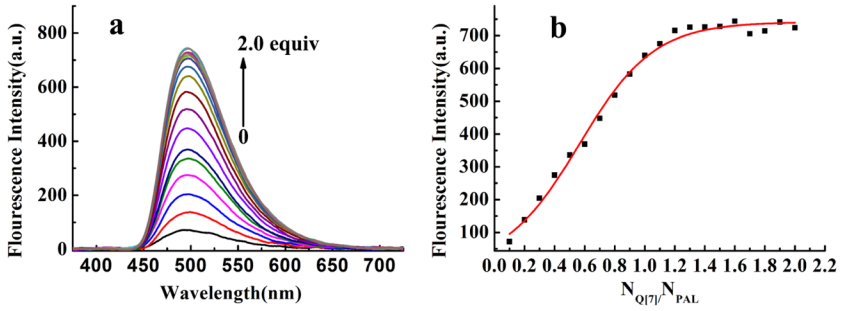

Fig. 4. (a) Fluorescence titration of PAL (2×10^{-5} mol·L^{-1}) with increasing concentrations of Q[7]; (b) absorbance (A) *vs.* ratio of number of mol of host and guest $N_{Q[7]}/N_{PAL}$.

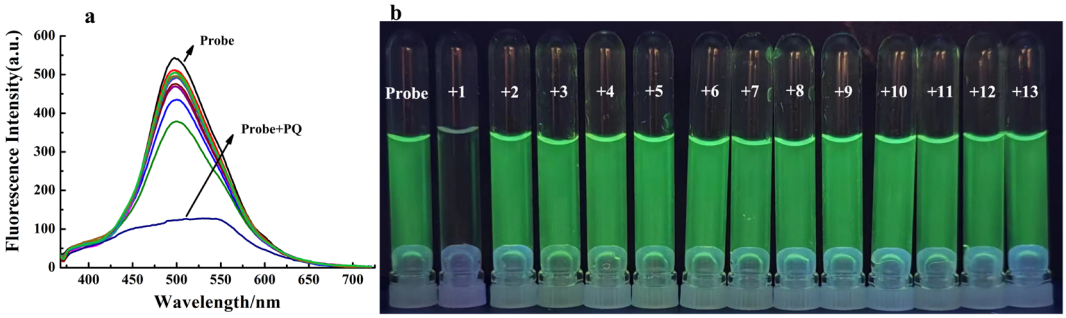

Fig. 5. (a) Fluorescence spectra of Q[7]/PAL in the presence of different pesticides in aqueous solution with λ_{ex}=343 nm; (b) Photographs of the different pesticides added in Q[7]/PAL under exposure to UV light (365 nm); (1 for Paraquat; 2 for Metalaxyl, 3 for Tricyclazole, 4 for Pyroquilon, 5 for Dodine, 6 for Pyrimethanil, 7 for Dinotefuran, 8 for Thiamethoxam, 9 for Pymetrozine, 10 for Acetamiprid, 11 for Metoxazon, 12 for Ethiofencarb, 12 for Hymexazol).

4. MALDI-TOF mass spectrometry

MALDI-TOF mass spectrometry is a technique commonly employed for the observation of host-guest interactions. As depicted in Fig. S4, a strong signal is observed at *m*/*z* 1515.52, which compares favorably with the calculated value of *m*/*z* 1514.50. This data further supports the formation of a 1:1 Q[7]/PAL host-guest inclusion complex.

5. Fluorescence quenching of Q[7]/PAL by PQ

As highlighted above, there is no intrinsic fluorescence in aqueous solution associated with PAL, whilst a fairly intense fluorescence occurs when PAL is in the presence of Q[7]. Given this, there is potential for this system to be employed for the identification of common pesticides. From the fluorescence measurements, it was clear that this system exhibited selectivity toward the pesticide PQ. In particular, fluorescence quenching was observed on addition of PQ (1×10^{-4} mol·L^{-1}) to the 1:1 inclusion complex comprising Q[7] (2×10^{-5} mol·L^{-1}) and PAL (2×10^{-5} mol·L^{-1}). By contrast, there was no significant fluorescence change when any of the other 12 pesticides (1×10^{-4} mol·L^{-1}) shown in Fig. S1 and named in the caption for Fig. 5 below were employed instead of PQ. These observations reveal that in aqueous solution, the selective detection of PQ can be achieved by employing the inclusion complex PAL@Q[7].

6. Effect of PQ concentration on the fluorescence intensity of the Q[7]/PAL system

The effect of different PQ concentrations on the fluorescence intensity of the complex PAL@Q[7] was next studied. As depicted in Fig. 6a, on increasing the concentration of PQ, the fluorescence intensity of the inclusion complex PAL@Q[7] slowly decreases. The corresponding fluorescence intensity of the PAL@Q[7] inclusion complex for a PQ concentration of 0–2.2×10^{-5} mol·L^{-1} is shown in Fig. 6b.

As is evident from Fig. S5, a near linear relationship is found for the value of the change in fluorescence intensity (ΔI) *versus* the concentration of PQ over a range of concentrations. The linear range is 0–1.2×10^{-5} mol·L^{-1}, and the linear regression equation is ΔI=36.7950C–44.1810 (C represents the concentration (mol·L^{-1}) of PQ) with a correlation coefficient of 0.9903, indicative of good linearity. The detection limit for PQ was calculated at 3.26×10^{-7} mol·L^{-1}.

7. The response mechanism of the fluorescent quenching

To gain an understanding of the reaction mechanism for the fluorescence quenching when PQ is added to Q[7]/PAL, NMR spectroscopic titration experiments were performed. In Fig. 7, the proton peaks associated with both PQ pyridine rings exhibited high field shifts (*versus* free PQ) when the PQ was added

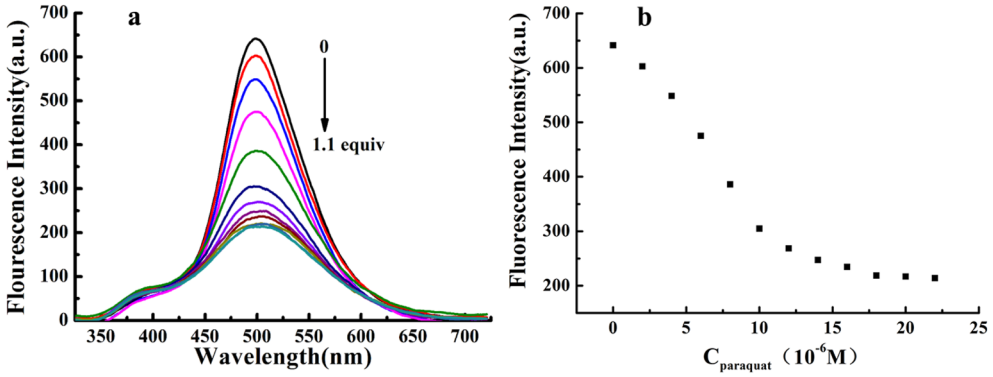

Fig. 6. (a) The fluorescence spectra of Q[7]/PAL at different PQ concentrations in aqueous solution with λ=343 nm; (b) The corresponding fluorescence intensity of the inclusion complex PAL@Q[7] when the concentration of PQ is varied from 0 to 2.2×10^{-5} mol·L^{-1}.

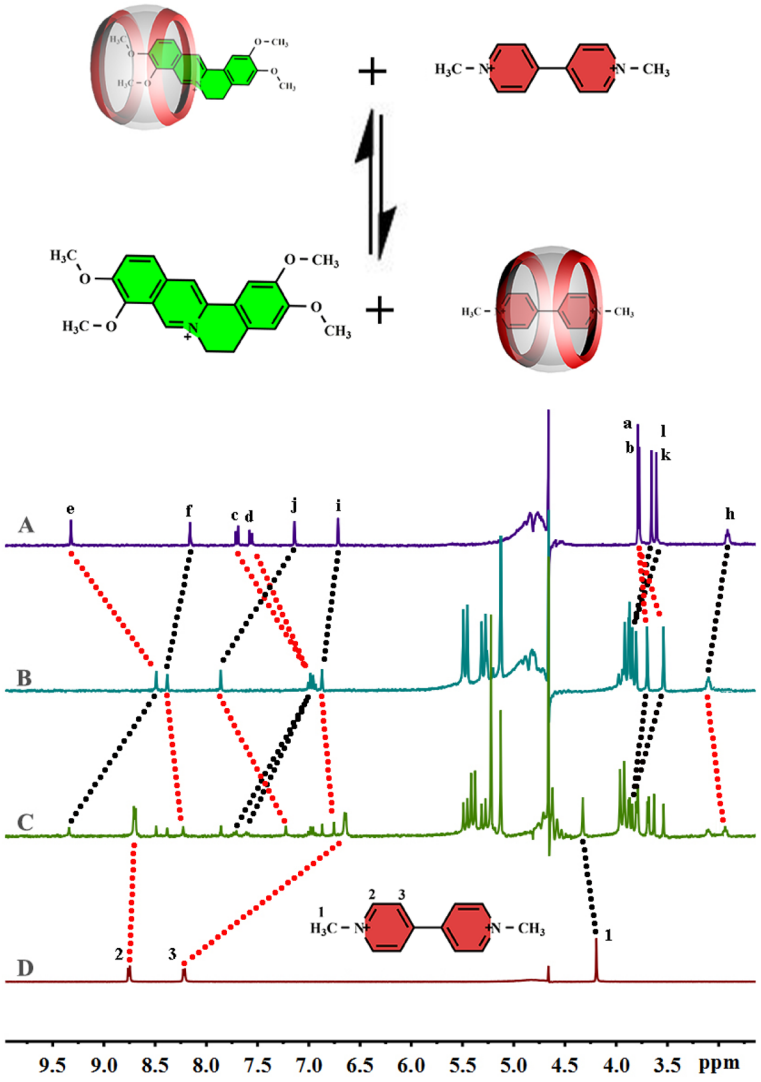

Fig. 7. ^{1}H NMR spectra of (A) PAL; (B) Q[7]/PAL host–guest system; (C) Q[7]/PAL/PQ system; (D) PQ.

Q[7]@PAL in D_2O. These observations are consistent with PQ buried within the Q[7] cavity, *i.e.*, formation of Q[7]@PQ with the PAL having been released (the PAL protons move to lower field).

Based on the reported literature,[46] in the structure of PAL, the isoquinoline ring and dimethoxy benzene are unable to form a conjugated system due to their connection *via* a six-membered ring, which results in PAL itself being non-fluorescent. However, upon encapsulation of PAL by a Q[7] cavity, there is an electrostatic attraction between the positive charge of the heterocyclic nitrogen of the PAL guest and the high-density electron cloud of the carbonyl oxygen on the main body. This effectively forms a conjugation system between the isoquinoline ring and dimethoxy benzene, which results in increased fluorescence intensity. An additional factor favorable for fluorescence enhancement is the reduced freedom of motion of PAL when it is embedded in the hydrophobic cavity of Q[7], which decreases the probability of the radiation-free jump. The enhanced fluorescence will be quenched when the PAL is replaced by other molecules. In this titration study, a significant increase of fluorescence results from the formation of the 1 : 1 host–guest complex when 1.0 eq of PAL was encapsulated by 1.0 eq of Q[7]. By contrast, when PQ was combined with the Q[7]/PAL host–guest system, PQ competitively occupies the Q[7] cavity. As can be seen from the ^{1}H NMR spectra, the peaks of the protons H2, H3 associated with the PQ were shifted to higher field relative to those of free PQ. This indicated that the PQ was located inside the Q[7] cavity (Fig. 7 and Fig. S6), whilst the movement downfield and broadening of the protons associated with PAL was consistent with one included PAL molecule being replaced by the PQ molecule, thereby forming a 1 : 1 inclusion complex. This provided a stable inclusion complex that led to fluorescence quenching, whereas the remaining 12 pesticides screened herein could not replace PAL and thus no significant change in fluorescence was observed. The method proposed in this paper can be compared with other methods reported in the analytical literature, as shown in Table

Table 1. Comparison of the Different Methods Used for PQ Detection

Method	Pesticide	Linear range	LOD	Ref
p-DPD@azoCX[4] probe	PQ	0.35–8.0 *u*M	0.35 *u*M	54)
Pillar[5]arene sensor	PQ	1 *u*M–0.1 M	0.22 *u*M	55)
Q[8]@dye array	PQ	0–26.0 *u*M	0.80 *u*M	56)
Q[7]@PAL sensor	PQ	0–12.0 *u*M	0.34 *u*M	This work

1.[56–58] The results show that the sensitivity of this method is equivalent to that of other methods and has a certain degree of specificity.

Conclusions

In this paper, the ability of Q[7] to bind with PAL in aqueous solution has been evaluated by a number of experimental methods, which confirmed that the PAL guest can be encapsulated in the Q[7] cavity to form a stable 1 : 1 host–guest inclusion complex. The resulting inclusion complex PAL@Q[7] in aqueous solution exhibits moderate intensity fluorescence. It is noteworthy that quenching of the fluorescence of the inclusion complex was evident following PQ addition, whilst the addition of any of the other 12 pesticides failed to result in any significant change in fluorescence. Thus, a new fluorescent probe with high sensitivity and selectivity for the determination of the herbicide PQ in aqueous solution has been developed. This study provides a new idea for the construction of fluorescent probes based on Q[*n*]s and a new method for the future detection of trace pollutants in water.

Acknowledgements

This work was financially supported by the Science and Technology Fund of Guizhou Province (ZK[2023]General 040 and ZK[2022]General 552). CR thanks the EPSRC for an Overseas Travel Grant (EP/R023816/1) for support.

Conflict of Interest

The authors declare that there are no conflicts of interest.

Electronic supplementary materials

The online version of this article contains supplementary materials (Supplemental Fig. S1, Fig. S2, Fig. S3, Fig. S4, Fig. S5, Fig. S6), which are available at https:// www.jstage.jst.go.jp/browse/jpestics/.

References

1) G. Aragay, F. Pino and A. Merkoçi: Nanomaterials for sensing and destroying pesticides. *Chem. Rev.* **112**, 5317–5338 (2012).
2) R. Gao, N. Choi, S. I. Chang, S. H. Kang, J. M. Song, S. I. Cho, D. W. Lim and J. Choo: Highly sensitive trace analysis of paraquat using a surface-enhanced Raman scattering microdroplet sensor. *Anal. Chim. Acta* **681**, 87–91 (2010).
3) N. Kamkrua, T. Ngernsutivorakul, S. Limwichean, P. Eiamchai, C. Chananonnawathorn, V. Pattanasetthakul, R. Ricco, K. Choowongkomon, M. Horprathum, N. Nuntawong, T. Bora and R. Botta: Au nanoparticle-based surface-enhanced raman spectroscopy aptasensors for paraquat herbicide detection. *ACS Appl. Nano Mater.* **6**, 1072–1082 (2023).
4) N. Li, M. Zhang, X. Geng, R. Liu, X. Meng, W. Zou, W. Chen, H. Shao and C. Wang: Rapid and highly sensitive determination of unexpected diquat and paraquat in biological fluids by electro-enhanced SPME-SERS. *Sens. Actuators B Chem.* **382**, 133504 (2023).
5) H. Wang, E. Hou, N. Xu, P. Nie, L. Chang, J. Wu and X. Zhang: Graphene electrochemical transistors decorated by Ag nanoparticles exhibiting high sensitivity for the detection of paraquat over a wide concentration range. *Anal. Methods* **15**, 959–968 (2023).
6) C. T. Hsieh, P. Y. Sung, Y. A. Gandomi, K. S. Khoo and J. K. Chang: Microwave synthesis of boron- and nitrogen-codoped graphene quantum dots and their detection to pesticides and metal ions. *Chemosphere* **318**, 137926 (2023).
7) Y. Xiong, T. Ma, H. Zhang, L. Qiu, S. Chang, Y. Yang and F. Liang: Gold nanoparticle functionalized nanopipette sensors for electrochemical paraquat detection. *Mikrochim. Acta* **189**, 251 (2022).
8) Z. Kang, J. Yang, J. Jiang, L. Zhao, Y. Zhang, Q. Tu, J. Wang and M.-S. Yuan: Pillar[5]arenes modified tetraphenylethylene as fluorescent chemosensor for paraquat detection. *Sens. Actuators B Chem.* **370**, 132436 (2022).
9) S. Sain, S. Roy, A. Mathur, V. M. Rajesh, D. Banerjee, B. Sarkar and S. S. Roy: Electrochemical sensors based on flexible laser-induced graphene for the detection of paraquat in water. *ACS Appl. Nano Mater.* **5**, 17516–17525 (2022).
10) R. Rajendran and L. Neelakantan: Recent advances in estimation of Paraquat using various analytical techniques: A review. *Results Chem.* **5**, 100703 (2023).
11) M. Liu, R. Cen, J. S. Li, Q. Li, Z. Tao, X. Xiao and L. Isaacs: Double-cavity nor-seco-cucurbit[10]uril enables efficient and rapid separation of pyridine from mixtures of toluene, benzene, and pyridine. *Angew. Chem. Int. Ed.* **61**, e202207209 (2022).
12) D. Yang, X. N. Yang, M. Liu, L. X. Chen, Q. Li, H. Cong, Z. Tao and X. Xiao: Cucurbit[5]uril-based porous polymer material for removing organic micropollutants in water. *Microporous Mesoporous Mater.* **341**, 112023 (2022).
13) A. E. Kaifer: Toward reversible control of cucurbit[*n*]uril complexes. *Acc. Chem. Res.* **47**, 2160–2167 (2014).
14) W. Zhang, Y. Luo, J. Zhao, C. Zhang, X.-L. Ni, Z. Tao and X. Xiao: Controllable fabrication of a supramolecular polymer incorporating twisted cucurbit[14]uril and cucurbit[8]uril *via* self-sorting. *Chin. Chem. Lett.* **33**, 2455–2458 (2022).
15) Q. Li, S.-C. Qiu, J. Zhang, K. Chen, Y. Huang, X. Xiao, Y. J. Zhang, F. Li, Y.-Q. Zhang, S.-F. Xue, Q.-J. Zhu, Z. Tao, L. F. Lindoy and G. Wei: Twisted cucurbit[*n*]urils. *Org. Lett.* **18**, 4020–4023 (2016).
16) X.-J. Cheng, L.-L. Liang, K. Chen, N.-N. Ji, X. Xiao, J.-X. Zhang, Y.-Q. Zhang, S.-F. Xue, Q.-J. Zhu, X.-L. Ni and Z. Tao: Twisted cucurbit[14]uril. *Angew. Chem. Int. Ed.* **52**, 7252–7255 (2013).
17) Y. Luo, W. Zhang, Q. Ren, Z. Tao and X. Xiao: Highly efficient artificial light-harvesting systems constructed in an aqueous solution based on twisted cucurbit[14]uril. *ACS Appl. Mater. Interfaces* **14**, 29806–29812 (2022).
18) R. H. Gao, Y. Huang, K. Chen and Z. Tao: Cucurbit[*n*]uril/metal ion complex-based frameworks and their potential applications. *Coord. Chem. Rev.* **437**, 213741 (2021).
19) Y. Luo, W. Zhang, M. X. Yang, X. H. Feng, C. Redshaw, Q. Li, Z. Tao and X. Xiao: A twisted cucurbit[14]uril-based fluorescent supramolecular polymer mediated by metal ion. *Macromolecules* **55**, 1642–1646 (2022).
20) W. Zhang, Y. Luo, C. Liu, M. X. Yang, J. X. Gou, Y. Huang, X. L. Ni, Z. Tao and X. Xiao: Supramolecular room temperature phosphorescent

materials based on cucurbit[8]uril for dual detection of dodine. *ACS Appl. Mater. Interfaces* **14**, 51429–51437 (2022).
21) M.-S. Li, M. Quan, X.-R. Yang and W. Jiang: Cucurbit[*n*]urils (n=7, 8) can strongly bind neutral hydrophilic molecules in water. *Sci. China Chem.* **65**, 1733–1740 (2022).
22) Y. Luo, W. Zhang, X. N. Yang, M. X. Yang, W. Min, Z. Tao and X. Xiao: Cucurbit[10]uril-based orthogonal supramolecular polymers with host-guest and coordination interactions and its applications in anion classification. *Inorg. Chem.* **61**, 16678–16684 (2022).
23) T. T. Zhang, X. N. Yang, J. H. Hu, Y. Luo, H. J. Liu, Z. Tao, X. Xiao and C. Redshaw: New dual-mode orthogonal tunable fluorescence systems based on cucurbit[8]uril: White light, 3D printing, and anti-counterfeit applications. *Chem. Eng. J.* **452**, 138960 (2023).
24) D. Yang, M. Liu, X. Xiao, Z. Tao and C. Redshaw: Polymeric self-assembled cucurbit[*n*]urils: Synthesis, structures and applications. *Coord. Chem. Rev.* **434**, 213733 (2021).
25) M. Liu, L. X. Chen, P. H. Shan, C. J. Lian, Z. H. Zhang, Y. Q. Zhang, Z. Tao and X. Xiao: Pyridine detection using supramolecular organic frameworks incorporating cucurbit[10]uril. *ACS Appl. Mater. Interfaces* **13**, 7434–7442 (2021).
26) W. Zhang, Y. Luo, X.-L. Ni, Z. Tao and X. Xiao: Two-step, sequential, efficient, artificial light-harvesting systems based on twisted cucurbit[14]uril for manufacturing white light emission materials. *Chem. Eng. J.* **446**, 136954 (2022).
27) P. H. Shan, J. H. Hu, M. Liu, Z. Tao, X. Xiao and C. Redshaw: Progress in host–guest macrocycle/pesticide research: Recognition, detection, release and application. *Coord. Chem. Rev.* **467**, 214580 (2022).
28) Z. Hirani, H. F. Taylor, E. F. Babcock, A. T. Bockus, C. D. Varnado Jr., C. W. Bielawski and A. R. Urbach: Molecular recognition of methionine-terminated peptides by cucurbit[8]uril. *J. Am. Chem. Soc.* **140**, 12263–12269 (2018).
29) W. Zhang, Y. Luo, P. H. Zhu, X. L. Ni, C. Redshaw, Z. Tao and X. Xiao: Supramolecular polymeric material based on twisted cucurbit[14]uril: Sensitive detection and removal of potential cyanide from water. *ACS Appl. Mater. Interfaces* **14**, 37068–37075 (2022).
30) Y. X. Chang, Y. Q. Qiu, L. M. Du, C. F. Li and M. Guo: Determination of ranitidine, nizatidine, and cimetidine by a sensitive fluorescent probe. *Analyst* **136**, 4168–4173 (2011).
31) Y. X. Chang, X. C. Duan, X. M. Zhang, F. Liu and L. M. Du: A new fluorometric method for the determination of oxaliplatin based on cucurbit[7]uril supramolecular interaction. *Aust. J. Chem.* **70**, 677–682 (2017).
32) R. Cen, M. Liu, H. Xiao, H. P. Yang, L. X. Chen, Q. Li, C. H. Wang, Z. Tao and X. Xiao: A double-cavity nor-seco-cucurbit[10]uril-based fluorescent probe for detection of ClO^- and its application in cell imaging. *Sens. Actuators B Chem.* **378**, 133126 (2023).
33) Y. Fan, R. H. Gao, Y. Huang, B. Bian, Z. Tao and X. Xiao: Supramolecular fluorescence probe based on twisted cucurbit[14]uril for sensing fungicide flusilazole. *Front Chem.* **7**, 154 (2019).
34) W. Zhang, Y. Luo, Y. Zhou, M. Liu, W. T. Xu, B. Bian, Z. Tao and X. Xiao: A highly selective fluorescent chemosensor probe for detection of Fe^{3+} and Ag^+ based on supramolecular assembly of cucurbit[10]uril with a pyrene derivative. *Dyes Pigments* **176**, 108235 (2020).
35) T. A. Martyn, J. L. Moore, R. L. Halterman and W. T. Yip: Cucurbit[7]uril induces superior probe performance for single-molecule detection. *J. Am. Chem. Soc.* **2007**, 10338–10339 (2007).
36) J. He, X. Y. Yu, Z. C. Yu, M. Liu, P. H. Shan, C. Redshaw, Y. Huang, Z. Tao and X. Xiao: Facile fluorescent detection of *o*-nitrophenol by a cucurbit[8]uril-based supramolecular assembly in aqueous media. *Anal. Chim. Acta* **1226**, 340262 (2022).
37) G. Y. Jiang, W. P. Zhu, Q. Q. Chen, X. B. Li, G. X. Zhang, Y. D. Li, X. L. Fan and J. G. Wang: Selective fluorescent probes for spermine and 1-adamantanamine based on the supramolecular structure formed between AIE-active molecule and cucurbit[*n*]urils. *Sens. Actuators B Chem.* **261**, 602–607 (2018).
38) D. Rosa-Gastaldo, A. Scopano, M. Zaramella and F. Mancin: Nanoscale supramolecular probes for the naked-eye detection of illicit drugs. *ACS Appl. Nano Mater.* **3**, 9616–9621 (2020).
39) W. Zhang, L. Yang, Y. Luo, H. Xiao, H. Yang, X. Ni, Z. Tao and X. Xiao: AIE biofluorescent probe based on twisted cucurbit[14]uril for the detection of $Fe(CN)_6^{3-}$ anion in solutions and live kidney cells. *Sens. Actuators B Chem.* **379**, 133255 (2023).
40) Q. Tang, J. Zhang, T. Sun, C. H. Wang, Y. Huang, Q. D. Zhou and G. Wei: A turn-on supramolecular fluorescent probe for sensing benzimidazole fungicides and its application in living cell imaging. *Spectrochim. Acta A Mol. Biomol. Spectrosc.* **191**, 372–376 (2018).
41) Y. J. Cao, S. Wang, W. Wu, H. Peng, Y. Yu and D. B. Zhu: Cucurbit[6]uril modified CdTe quantum dots fluorescent probe and its selective analysis of p-nitroaniline in environmental samples. *Talanta* **199**, 667–673 (2019).
42) W. T. Xu, H. M. Feng, W. W. Zhao, C. H. Huang, C. Redshaw, Z. Tao and X. Xiao: Amino acid recognition by a fluorescent chemosensor based on cucurbit[8]uril and acridine hydrochloride. *Anal. Chim. Acta* **1135**, 142–149 (2020).
43) Z. S. Zeng, Y. Q. Zhang, X. D. Zhang, G. Y. Luo, J. Xie, Z. Tao and Q. J. Zhang: Selective detection of Zn^{2+} and Cd^{2+} ions in water using a host-guest complex between chromone and Q. *Chin. Chem. Lett.* **32**, 2572–2576 (2021), 7.
44) H. Wu, J. Zhao, X. N. Yang, D. Yang, L. X. Chen, C. Redshaw, L. G. Yang, Z. Tao and X. Xiao: A cucurbit[8]uril-based probe for the detection of the pesticide tricyclazole. *Dyes Pigments* **199**, 110076 (2022).
45) Y. Li, C. F. Li, L. M. Du, J. X. Feng, H. L. Liu and Y. L. Fu: A competitive strategy based on cucurbit[7]uril supramolecular interaction for simple and sensitive detection of dibucaine. *Talanta* **132**, 653–657 (2015).
46) J. Y. Yang, L. M. Du, H. Wu, Y. X. Chang and C. F. Li: Determination of L-Cystine by a new sensitive cucurbit[7]uril/palmatine probe. *Chin. J. Chem.* **29**, 1268–1272 (2011).
47) P. H. Shan, J. Zhao, X. Y. Deng, R. L. Lin, B. Bian, Z. Tao, X. Xiao and J. X. Liu: Selective recognition and determination of phenylalanine by a fluorescent probe based on cucurbit[8]uril and palmatine. *Anal. Chim. Acta* **1104**, 164–171 (2020).
48) P. H. Shan, J. L. Kan, X. Y. Deng, C. Redshaw, B. Bian, Y. Fan, T. Zhu and X. Xiao: A fluorescent probe based on cucurbit[7]uril for the selective recognition of phenylalanine. *Spectrochim. Acta A Mol. Biomol. Spectrosc.* **233**, 118177 (2020).
49) C. Li, J. Li and X. Jia: Selective binding and highly sensitive fluorescent sensor of palmatine and dehydrocorydaline alkaloids by cucurbit[7]uril. *Org. Biomol. Chem.* **7**, 2699–2703 (2009).
50) H. M. Zhang, J. Y. Yang, L. M. Du, C. F. Li and H. Wu: Determination of sotalol by fluorescence quenching method. *Anal. Methods* **3**, 1156–1162 (2011).
51) K. Yan, L. C. Wang, H. M. Zhou, Z. D. Hua, P. Xu, H. Xu, Y. M. Wang, B. Di and C. Hu: Cucurbituril-mediated AIE: An unconventional indicator displacement assay for ketamine detection. *Dyes Pigments* **197**, 109875 (2022).
52) Y. Ling, J. T. Mague and A. E. Kaifer: Inclusion Complexation of Diquat and Paraquat by the Hosts Cucurbit[7]uril and Cucurbit[8]uril. *Chemistry* **13**, 7908–7914 (2007).

53) J. Kim, I. S. Jung, S. Y. Kim, E. Lee, J. K. Kang, S. Sakamoto, K. Yamaguchi and K. Kim: New cucurbituril homologues: Syntheses, isolation, characterization, and X-ray crystal structures of cucurbit[*n*]uril (n=5, 7, and 8). *J. Am. Chem. Soc.* **122**, 540–541 (2000).
54) C. X. Zhang, X. Jing, L. M. Du, H. L. Liu, J. Li, S. G. Zhao and Y. L. Fu: Cucurbit[7]uril host–guest complexation of nereistoxin investigated by competitive binding of palmatine fluorescent probe. *Prog. React. Kinet. Mech.* **40**, 154–162 (2015).
55) Z. Miskolczy, M. Megyesi, O. Toke and L. Biczók: Change of the kinetics of inclusion in cucurbit[7]uril upon hydrogenation and methylation of palmatine. *Phys. Chem. Chem. Phys.* **21**, 4912–4919 (2019).
56) T. Jia, C. Pu, T. Qin, B. Liu, G. Yao, Z. Xun, B. Wang, Y. Tian, Z. Zhang, H. Xu and C. Zhao: Azocalixarene-based supramolecular system for the detection of paraquat *via* an improved indicator displacement assay. *J. Agric. Food Chem.* **70**, 15981–15989 (2022).
57) Z. Zhao, F. Zhang and Z. Zhang: A facile fluorescent "turn-off" method for sensing paraquat based on pyranine–paraquat interaction. *Spectrochim. Acta A Mol. Biomol. Spectrosc.* **199**, 96–101 (2018).
58) T. Wiwasuku, A. Chuaephon, U. Habarakada, J. Boonmak, T. Puangmali, F. Kielar, D. J. Harding and S. Youngme: A water-stable lanthanide-based MOF as a highly sensitive sensor for the selective detection of paraquat in agricultural products. *ACS Sustain. Chem.& Eng.* **10**, 2761–2771 (2022).